J Plant Growth Regul (2016) 35:316–329
DOI 10.1007/s00344-015-9535-4

Transcriptome Sequencing Determined Flowering Pathway Genes in *Aechmea fasciata* Treated with Ethylene

Zhiying Li[1,2] · Jiabin Wang[1,2] · Xuequan Zhang[1,2] · Ming Lei[1,2] · Yunliu Fu[1,2] · Jing Zhang[1,2] · Zhi Wang[1,2] · Li Xu[1,2]

Received: 18 January 2015 / Accepted: 22 June 2015 / Published online: 26 August 2015

Abstract *Aechmea fasciata* is a well-known ornamental flowering plant in the bromeliad family. It is proposed that a small burst of ethylene synthesis in the meristem triggers flowering in pineapple and other bromeliads in response to diverse environmental and endogenous signals. *A. fasciata* showed an age-dependent response: adult plants were induced to flower successfully under ethylene treatment but juvenile plants did not. To better understand the mechanism of different responses to ethylene in transcriptome and flowering induction by ethylene, we performed a comparative analysis of *A. fasciata* transcriptome. Four libraries of *A. fasciata* adult and juvenile plants under water and ethylene treatment were sequenced by Illumina deep sequencing, 55,238,936, 53,797,292, 53,471,812, and 53,485,862 qualified Illumina clean reads, respectively, with 90 bp mean length, respectively. Unigenes of the four libraries were assembled and then merged into an unified library with 86,609 sequences and a mean size of 987 bp. After searching against Nr, KEGG, Swiss-Prot, and COG databases, 28,350 sequences were assigned to 129 KEGG pathways, 28,289 unigenes were categorized into 64 functional groups, and 19,293 sequences were classified into 25 COG categories. Through differential expression analysis, 56 DEGs related to flowering were identified. The critical genes correlated with flowering were selected and confirmed by qRT-PCR analysis. This study provided a global survey of changes in transcriptomes of *A. fasciata* in response to ethylene. The analyses of transcriptome profiles imply that *FT* is upregulated in the adult plant and results in flowering. Moreover, the differential expression of *GI*, *DELLA*, *GAD1*, *AP2,* and so on indicated that a complicated network participated in the induction of flowering by ethylene, which will help in the future studies.

Keywords *Aechmea fasciata* · Transcriptome · Flowering · Ethylene

Zhiying Li and Jiabin Wang have been contributed equally to this work.

Electronic supplementary material The online version of this article (doi:10.1007/s00344-015-9535-4) contains supplementary material, which is available to authorized users.

✉ Li Xu
xllzy@263.net

Zhiying Li
xllizhiying@vip.163.com

Jiabin Wang
jiabinwangfuhu@sina.com

Xuequan Zhang
quanxue2008@126.com

Ming Lei
leiming_cv@126.com

Yunliu Fu
fyljj_2007@126.com

Jing Zhang
1956732492@qq.com

Zhi Wang
569234222@qq.com

[1] Institute of Tropical Crop Genetic Resources, Chinese Academy of Tropical Agricultural Sciences, Danzhou 571737, Hainan, China

[2] Ministry of Agriculture Key Laboratory of Crop Gene Resources and Germplasm Enhancement in Southern China, Chinese Academy of Tropical Agricultural Sciences, Danzhou, China

Background

Aechmea fasciata is a well-known tropical flowering plant in the *bromeliad* family. It is proposed that a small burst of ethylene synthesis in the meristem triggers flowering in pineapple and other *bromeliads* in response to diverse environmental and endogenous signals (Trusov and Botella 2006). To control flowering time and improve flowering uniformity, ethylene and its alternatives have been used to induce flowering in large-scale industrial bromeliad production for a long time. Under ethylene treatment, *A. fasciata* showed an age-dependent response: adult plants were induced to flower successfully but juvenile plants were not (Jung and others 2012).

Plants monitor environmental and developmental changes through a sophisticated regulatory network to control the timing of flowering. A network of six major pathways that control flowering time was characterized in *Arabidopsis thaliana*, including the photoperiod and vernalization pathways in response to seasonal changes of day length and temperature, the ambient temperature pathway in response to daily temperature, and age, autonomous and gibberellin integrated physiological cues of plants (Fornara and others 2010). Recent studies indicated that *FlOWERING LOCUS T* (*FT*) expression by various factors including temperature, photoperiod, GA, and plant age was induced by transcriptional activator *CONSTANS* (*CO*) and triggered plant flowering (Andres and Coupland 2012). Light signaling and the circadian clock controlled the activity of *CO* protein (Andres and Coupland 2012). The circadian clock-regulated protein *GIGANTEA* (*GI*), a large nuclear protein, plays a key role in regulating *CO* expression (Song and others 2013). It has been reported that *GI* can trigger activation of *FT* directly in a *CO*-independent manner (Sawa and Kay 2011). The stability of *CO* protein is also controlled by blue light photoreceptor cryptochromes *CRY2*, through a tripartite complex formed by *CRY2*, *RING-finger E3 ubiquitin ligase CONSTITUTIVE PHOTOMORPHOGENESIS 1* (*COP1*) and *SUPRESSOR OF PHYA-105 1* (*SPA1*), repressing the activity of *COP1-SPA1* and leading to *CO* protein stabilization (Zuo and others 2011). GA affected flowering time through the control of *DELLA* protein stabilization. Bioactive GAs promote binding of the *GID1* receptor to *DELLA* and initiate *DELLA* degradation (Mutasa-Gottgens and Hedden 2009). *DELLA* reduces the expression of FT, acting as a negative regulator of the GA signaling pathway and flowering (Galvao and others 2012). *DELLA* attenuates the binding ability of phytochrome-interacting factor 4 (PIF4), which activates the expression of *FT* at high temperatures (Kumar and others 2012). *DELLA* also reduces the level of MicroRNA172 (miR172), delaying flowering partly (Yu and others 2012). *APETALA 2* (*AP2*), *TARGET OF EAT 1* (*TOE1*), *TARGET OF EAT 2* (*TOE2*), and *TARGET OF EAT 3* (*TOE3*), acting as floral repressors, are the targets of miR172 and downregulated by miR172 (Aukerman and Sakai 2003). The abundance of miR172 increases as plants develop, in the mean while, miR156 correlated negatively with the expression level of miR172 (Jung and others 2007). The miR156 targets are *SQUAMOSA PROMOTER BINDING PROTEIN-LIKE* (*SPL*) transcripts, of which *SPL9* activates the transcription of MIR172 and *SPL3* binds to promoter of *FT* to induce *FT* expression (Wu and others 2009). A few of transcription repressors such as *FLOWERING LOCUS C* (*FLC*), *SHORT VEGETATIVE PHASE* (*SVP*), and *TEMPRANILLO 1* (*TEM1*) bind to the *FT* locus (Song and others 2013). *FLC* plays a key role in vernalization and autonomous pathways, as well as in ABA and BRs mediating flower timing (Fornara and others 2010; Wang and others 2013). It is supposed that the floral repressors including *SVP*, *TEM1*, *AP2*, *TOE1*, *TOE2*, and *TOE3* regulated by development stages, prevent precocious flowering by repressing *FT* expression either under unsuitable conditions for flowering or in the juvenile developmental stages (Song and others 2013). After expression in the leaf, *FT* is transferred to the shoot apical meristem and interacts with bZIP transcription factor *FD*, promoting the expression of MADS-box factor *APEATELA1* (*AP1*) and initiating flower development.

Ethylene was considered an ‘aging’ hormone often because it promotes such developmental processes as senescence, abscission, and ripening, and it also promotes flowering in *Bromeliads* but inhibits it in others (Schaller 2012). The essential elements of the ethylene signaling pathway include the ethylene receptors such as *ETR1*, *ERS1*, *ETR2*, *ERS2*, and *EIN4*, the transmembrane protein *EIN2*, the Raf-like kinase *CTR1*, and the transcription factors *EIN3* and *EILs*. A signal triggered by ethylene is transduced via *CTR1* and *EIN2* to *EIN3/EILs*, which are the transcription factors localized in the nucleus and regulate a wide array of plant pathways (Merchante and others 2013). Of the key elements of the ethylene signaling pathway, the ethylene receptors and *CTR1* are negative regulators, while *EIN3* and *EILs* act as positive regulators (Hua and Meyerowitz 1998; Kieber and others 1993; Solano and others 1998). Multiple mechanisms for the ethylene-mediated plant developmental response have been identified, in which *EILs* and the downstream ethylene response DNA-binding factor (EDF) and ethylene response factor (ERF) play a key role (Chuck and Hake 2005; Lingam and others 2011; Schaller 2012; Zhong and others 2009). In *A. thaliana,* ethylene delays flowering by reducing bioactive GA levels and enhancing *DELLA* accumulation via *EIN3* (Achard and others 2007). But the mechanism for ethylene-

induced flowering in bromeliads remains unclear, though ethylene has been used to induce flowering in bromeliads for a long time.

In our previous study, we performed a comparative transcriptome analysis of *A. fasciata* juvenile and adult plants under ethylene treatment, and many differentially expressed genes (DEGs) related to flower development and ethylene signaling were indentified. However, it is hard to determine whether the differential expression level of DEGs detected above was in response to ethylene or due to the difference of development stages. To further detect the difference between adult plant and juvenile plant responses to ethylene and genes with regard to age-dependent flowering induction of *A. fasciata*, four transcriptome libraries of adult plants and juvenile plants under ethylene treatment and water treatment were sequenced and analyzed, which showed a meaningful result. Data of this experiment will guide future studies on mechanisms of flowering induction by ethylene in bromeliads.

Methods

Plant Sample Preparation and RNA Isolation

A. fasciata juvenile (6–8 months) and adult (11–14 months) plants were collected from a greenhouse located in the experimental area at the Institute of Tropical Crop Genetic Resources, Chinese Academy of Tropical Agricultural Sciences (CATAS). *A. fasciata* plants were treated with 400 ul 1^{-1} of ethrel for 24 h (ambient temperature was 30–32 °C), and plants were also treated with water as a control. The shoot tip tissues and surrounding core leaves were physically isolated and immediately frozen in liquid nitrogen. Frozen tissues from each samples were ground to a fine powder using a mortar and pestle. Total RNA was extracted from the sample for 8 min at 65 °C using the CTAB extraction method. The RNA samples were treated with 10 units of DNaseI (Takara) for 30 min at 37 °C to remove the genomic DNA. The RNA quantity was examined using spectrophotometry, and the RNA quality was checked by gel electrophoresis.

Library Preparation for Transcriptome Analysis and Illumina Deep Sequencing

Using the OligoTex mRNA mini kit (Qiagen), poly-A-containing mRNAs were enriched from the total RNA samples. Then the mRNA was fragmented into small pieces using an RNA fragmentation kit (Ambion). These short fragments were used as the templates for cDNA synthesized. The double-stranded cDNA strand was synthesized using a double-stranded cDNA synthesis kit (Invitrogen). The cDNA fragments were purified using the QiaQuick PCR extraction kit (Qiagen) and eluted with EB buffer. The short cDNA fragments were then liganded with sequencing adapters, and the products were subsequently purified and amplified using PCR to prepare the final cDNA libraries. The four constructed cDNA libraries were then sequenced using Illumina HiSeq^{TM} 2000. The output raw reads were filtered by the trimming of adaptor sequences, empty reads, and ambiguous nucleotides ('N' in the end of the reads).

Functional Annotation and Classification

The Clean reads obtained were then assembled using the Trinity de novo transcriptome assembly software (Grabherr and others 2011). The core eukaryotic gene-mapping approach (CEGMA) was used to assess the completeness of the transcriptome assembly. Then, BLASTX alignments (e value $<$ 1e-5) between the unigenes were searched against protein databases, including Nr, Swiss-Prot, KEGG, and COG, and the best matched results were used to determine the sequence direction of the unigenes. Then, the ESTScan software was used to predict the coding regions and the sequence direction of unigenes that have no significant results in the search against protein databases above (Iseli and others 1999). The BLAST2GO program was applied to Gene Ontology analysis of unigenes using the best alignment results searched against the Nr database (Conesa and others 2005). Then the distribution of GO annotations was plotted by WEGO software (Livak and Schmittgen 2001). The KEGG and COG annotations were assigned using the searching result against KEGG and COG databases.

Unigene Expression Analysis

The Trinity toolkit was used to estimate the abundance of unigenes and indentify DEGs (Grabherr and others 2011). Reads of each library were mapped to the transcriptome assembly using bowtie with a maximum insert size of 800 (Langmead and others 2009). Using RSEM, the abundance of unigenes was estimated and assigned a FPKM value, and edgeR was used to identify DEGs (Mortazavi and others 2008; Pfaffl 2001; Robinson and others 2010). An FPKM filtering cut-off of 1.0 in at least one of the four libraries was used to determine expressed transcripts. When determining the DEGs, a cut-off of 1.0 in at least one the four libraries was used. Then DEGs were selected on the condition of p value ≤ 0.001 and $|\log2\ FC| \geq 1$. GO functional enrichment analysis was performed using GO-TermFinder (Boyle and others 2004). KEGG pathway enrichment was performed using KOBAS 2.0 (Mao and others 2005).

Quantitative Real-Time PCR (qRT-PCR) of RNA-Seq Data

The DEGs involved in flowering were selected for confirmation by qRT-PCR analysis. Total RNA was extracted from the shoot tip tissues and surrounding core leaves and used for cDNA synthesis with the same procedures as described above. Real-time PCR reactions were performed on buffer (10 μl) composed of 0.2 μM of gene-specific primers (Supplementary Data 1), 50 ng of cDNA samples and 5 μl of 2 × SYBR Green Master Mix Reagent (Applied Biosystems). The gene for actin was used as an internal control to estimate the relative expression level of the analyzed genes. The thermal cycles were set as follows: 95 °C for 10 min, and 45 cycles of 95 °C for 5 s, 60 °C for 30 s. The relative expression of genes was calculated using the delta–delta Ct method of the system (Livak and Schmittgen 2001). The corresponding qRT-PCR efficiencies were calculated according to the mathematical model of Pfaffl (Pfaffl 2001). The qRT-PCR products were validated by both sequencing and gel electrophoresis. The qRT-PCR reactions were set up with three biological replications and three technical replicates per experiment.

Results

Illumina Sequencing and De novo Assembly

In this study, four cDNA libraries from adult and juvenile plants under ethylene treatment and water treatment were prepared and subjected to Illumina deep sequencing (Fig. 1). The RNA integrity numbers (RIN) of the four libraries were determined by RNA samples bioanalyzer firstly, which generated the RIN scores of 8.3, 7.1, 7.6, and 6.9 for the four samples, respectively. The outputs of sequenced data from adult plants with water treatment (A0), juvenile plants with water treatment (J0), adult plants with ethylene treatment (A1), and juvenile plants with ethylene treatment (J1) were 55,238,936, 53,797,292, 53,471,812, and 53,485,862 qualified Illumina clean reads, respectively, with 90 bp mean length. These reads of the four libraries were assembled into unigene sequences using de novo assembly software trinity (Grabherr and others 2011). Then, Unigenes of the four libraries were merged into a unified library with 86,609 sequences and a mean size of 987 bp, which included all non-redundant unigene sequences of the four libraries (Table 1). Figure 2 shows the distribution of transcript lengths, which range from 200 to 11,534.

The CEGMA approach was used to assess the completeness of the transcriptome assembly, using a similarity search of the assembly with a set of 248 conserved eukaryotic core genes (CEGs) (Parra and others 2007). Of the 248 CEGs, 236 (95.16 %) genes are completely assembled and 247 (99.60 %) were partially assembled, indicating that the transcriptome assembly was of good completeness.

Functional Annotation

For annotation, unigene sequences of *A. fasciata* were first searched against the non-redundant (Nr) database of NCBI using BlastX with a cut-off *e* value of 1e-5. Of the searching results, 49,423 genes (57.06 % of unigene sequences) showed significant similarity to the proteins in the Nr database. The similarity distribution of the best matches is shown in Fig. 3a, 15.4 % of the matches were of high similarity ranging from 85 to 100, and 39.2 % of the hits were of similarity ranging from 60 to 80 %. Moreover, the species-based distribution of best matches is shown in the Fig. 3b. The result of homology analysis revealed that 18.47 % of the genes of *A. fasciata* showed the greatest similarity to *Oryza sativa Japonica Group*, while *Vitis vinifera* (13.99 %), *Sorghum bicolor* (9.91 %), *Brachypodium distachyon* (9.90 %), *Zea mays* (9.09 %), *Oryza sativa Indica Group* (6.00 %), and *Hordeum vulgare subsp. Vulgare* (3.82 %) showed a lower similarity to genes of *A. fasciata*. Then, these unigene sequences were searched against the Swiss-Prot database using a cut-off *e* value of 1e-5, with 35,251 genes (40.70 % of unigene sequences) returning an above cut-off BLAST result.

GO annotations were used to classify the functions of the unigene sequences based on the result of BlastX searching against the Nr database using blast2go (Conesa and others 2005). Among the unigenes with significant hits in searching against the Nr database, 28,289 unigenes were categorized into 64 functional groups (Supplementary Data 2). Among the sub-categories of three main GO categories, 'cell' (10.6 %), 'cell part' (10.6 %), 'organelle' (8.6 %), 'cellular process' (7.9 %), 'metabolic process' (7.7 %), 'catalytic activity' (7.0 %), 'binding' (7.0 %) were the most represented categories. Only a few unigenes were classified into the categories of 'virion,' 'viron part,' 'extracellular matrix part,' 'metallochaperone activity,' 'channel regulator activity,' 'protein tag,' and 'viral reproduction' (Fig. 4).

To further evaluate the completeness of our transcriptome library, we searched the annotated sequences against Clusters of Orthologous Group (COG) databases. In total, 19,293 sequences were assigned a COG classification (Fig. 5). These sequences were classified into 25 categories, of which the categories 'General function prediction only' (11.7 %), 'Translation,' 'ribosomal structure and biogenesis' (11.2 %), 'Transcription' (9.5 %), 'Replication, recombination and repair' (8.4 %), 'Function unknown' (8.3 %) were the top 5 categories

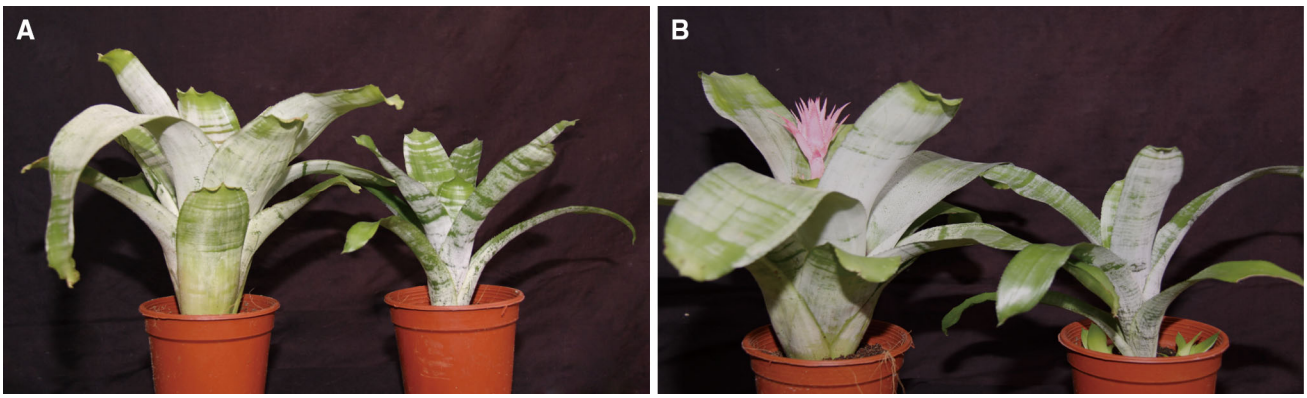

Fig. 1 *A. fasciata* juvenile and adult plants. **a** Adult plants (*right*) and juvenile plants (*left*), **b** adult plants (*right*) and juvenile plants (*left*) after ethylene treatment 40 days

Table 1 Summary of assembly and sequencing of *A. fasciata* transcriptome

		A0	J0	A1	J1
Clean reads	Total number	55,238,936	53,797,292	52,560,902	52,396,972
	Total nucleotides (nt)	4,971,504,240	4,841,756,280	4,730,481,180	4,715,727,480
Unigene	Total number	86,609			
	Total length (nt)	85,488,917			
	N50	1656			
	Mean length	987			

A0 adult plant with water treatment, *J0* juvenile plant with water treatment, *A1* adult plant with ethylene treatment, *J1* juvenile plant with ethylene treatment

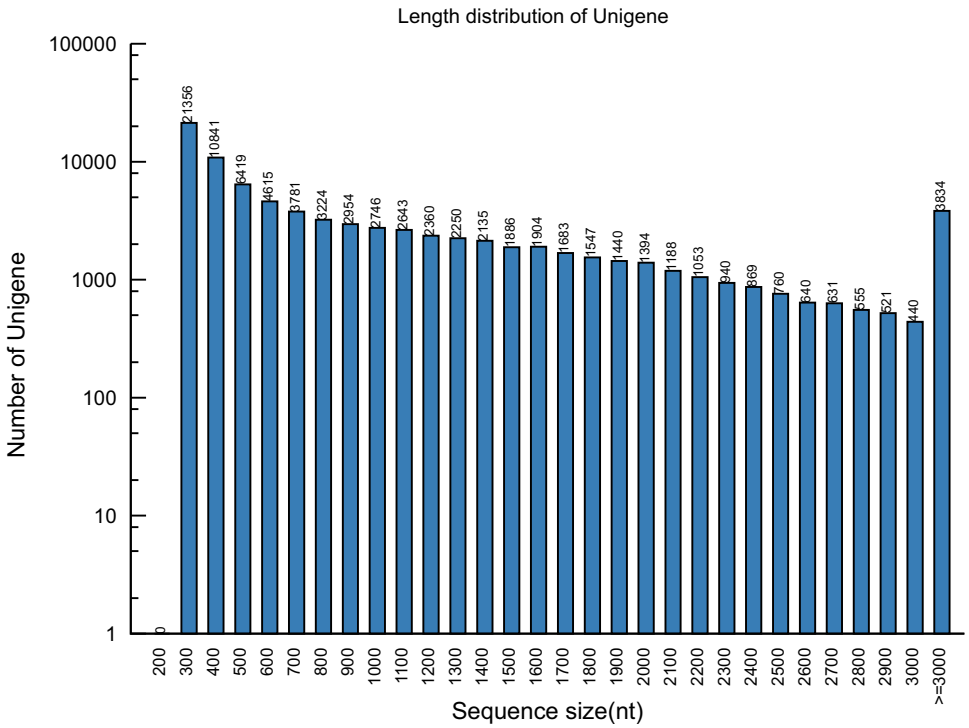

Fig. 2 The length distribution of assembled sequences. The reads from four libraries were assembled into 86,609 transcripts

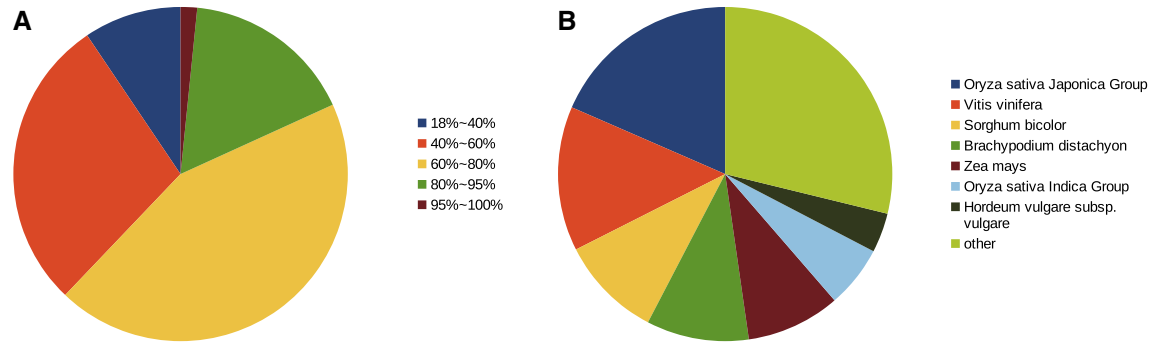

Fig. 3 Summary for results of BlastX against NCBI NR database. **a** Similarity distribution of BlastX results. **b** Species-based distributions of BlastX results

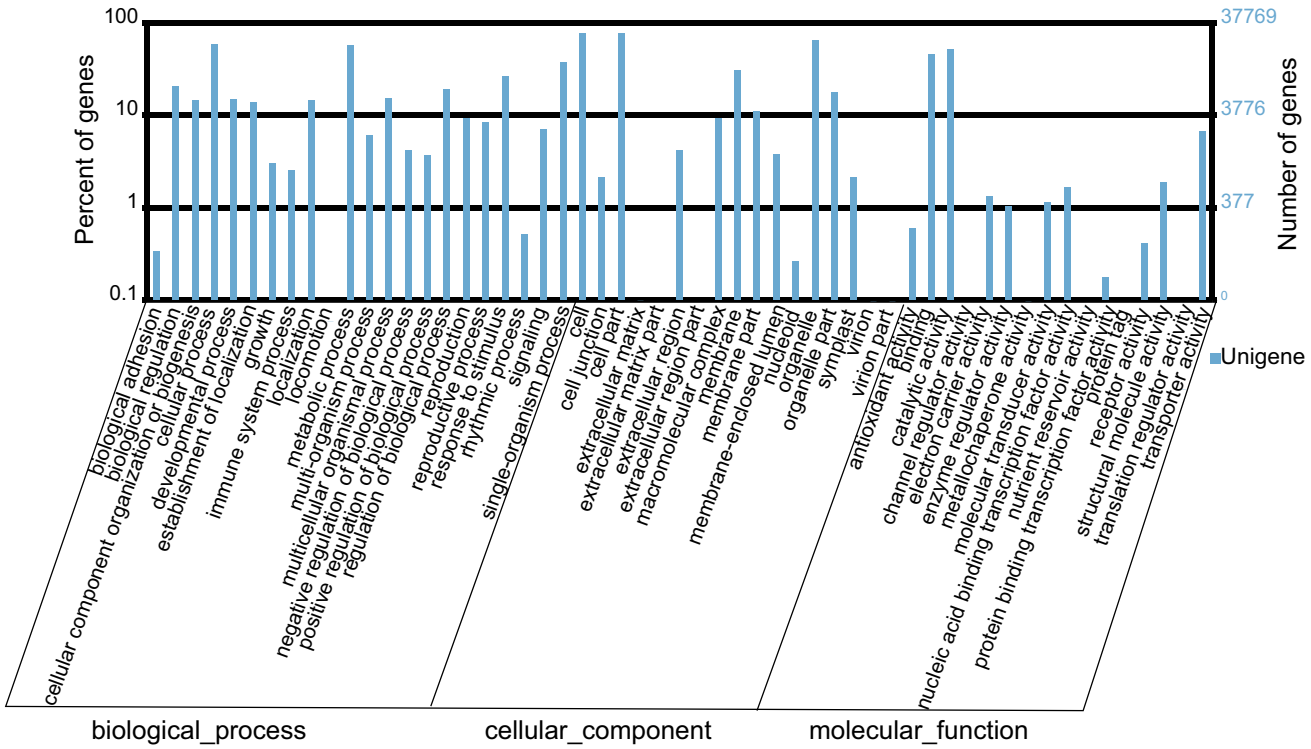

Fig. 4 GO assignments for transcriptome of *A. fasciata*

(Supplementary Data 3). Moreover, of the 25 categories, 'Defense mechanisms' (13; 0.023 %) and 'Nuclear structure' (2; 0.0036 %) were the least represented.

To identify the biological pathways that are active in *A. fasciata*, we mapped the unigene sequences to the reference canonical pathways in the Kyoto Encyclopedia of Genes and Genomes (KEGG). In total, we assigned 28,350 sequences to 129 KEGG pathways (Supplementary Data 4). Among the KEGG pathways, 'Metabolic pathways' (16.5 %), 'Spliceosome' (7.8 %), 'Biosynthesis of secondary metabolites' (5.4 %), 'Endocytosis' (4.4 %), 'RNA transport' (4.3 %), 'Ether lipid metabolism' (3.9 %), 'Plant-pathogen interaction' (3.6 %), and 'mRNA surveillance pathway' (3.2 %) were the highly represented pathways.

After a similarity search against transcription factor (TF) sequences in PlantTFDB using BlastX (*e* value < 1e-5), we identified 3347 putatively TFs (Jin and others 2013). These putatively TFs were assigned to 56 families according to the classification of TFs in Planttfdb (Supplementary Data 5). Among the TF gene families, bHLH (298) has the greatest number of transcripts, followed by C2H2 (233), MYB-related (215) and C3H (209). LFY (2), VOZ(3), and HRT-like (3) have fewer transcripts.

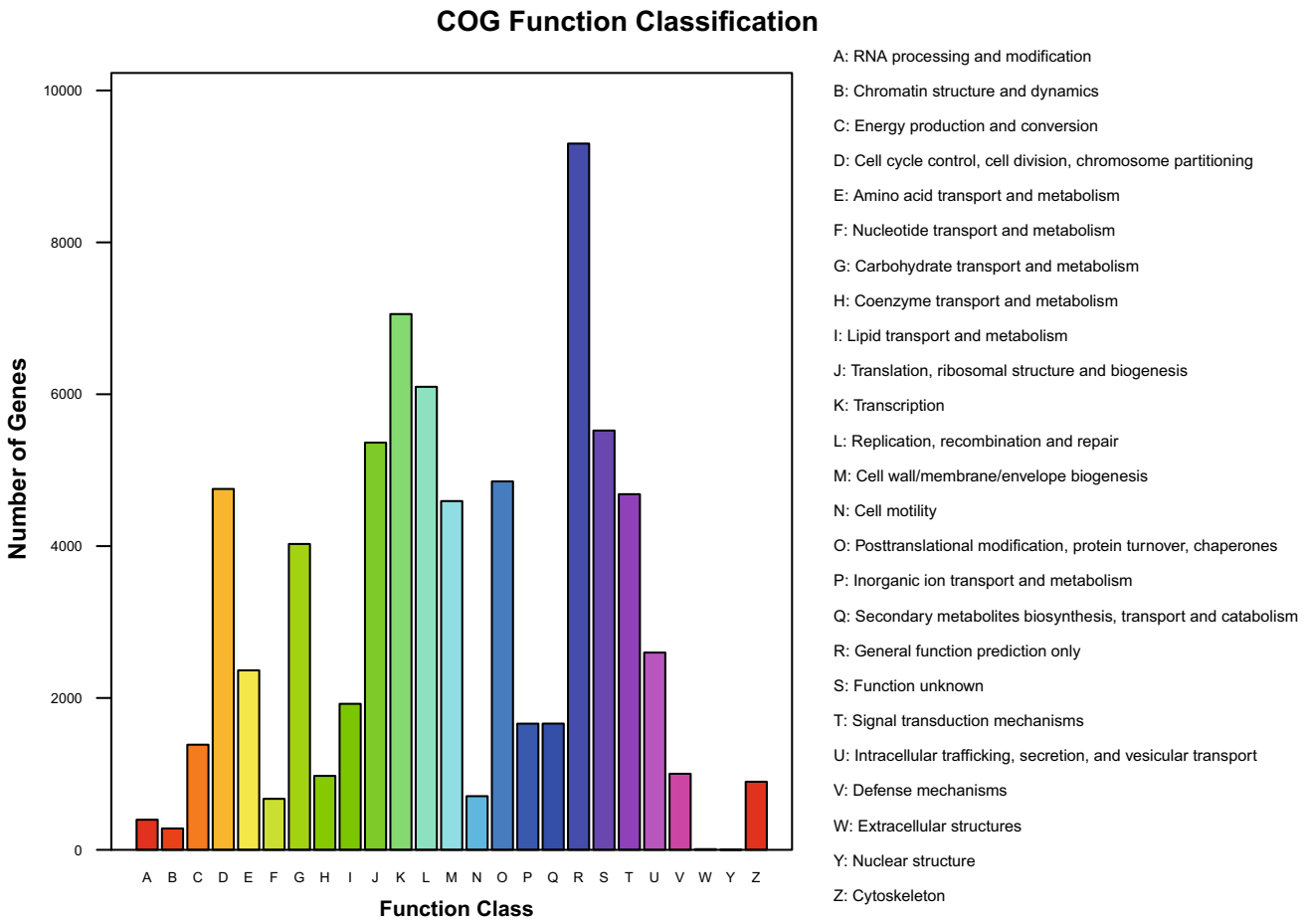

Fig. 5 COG Functional classification of transcriptome of *A. fasciata*

For the unigenes having no significant hits in searching against the protein databases above, the CDS of the unigenes are predicted by ESTScan (Iseli and others 1999) and then translated into peptide sequences. In the end, we obtained a "Blast-CDS" library with 49,538 unigene sequences and an 'ESTscan-CDS' library with 1499 EST sequences.

Unigene Expression Analysis

Expression analysis of four libraries was carried out using Trinity software. Clean reads from each library were mapped into merged transcriptome libraries. Then, the expression abundance of each gene was calculated and assigned a FPKM value. A total of 7748 DEGs were detected from the comparison of four libraries, of which 1231, 1328, 4879, and 3982 DEGs were identified from 'A0_vs_J0,' 'A1_vs_J1,' 'A0_vs_A1,' and 'J0_vs_J1,' respectively. The expression types of four libraries are shown in Fig. 6. As shown in Fig. 7, there were 671 upregulated genes and 651 downregulated genes for 'A0_vs_J0,' 787 upregulated genes and 444 downregulated genes for 'A1_vs_J1,' 1981 upregulated genes and 2898 downregulated for 'A0_vs_A1,' and 2084 upregulates genes and 1898 downregulated genes for 'J0_vs_J1,' respectively. We then investigated the distribution of DEGs in the TF gene families (Supplementary Data 5). Totally, 48 TF gene families had the number of DGEs ranging from 1 to 40. There were 13, 4, 23, 1, and 3 DEGs assigned into the TF gene families MIKC, CO-like, ERF, EIL, and AP2, respectively, which maybe involved in the regulation of flowering.

To further detect the function of DEGs, we performed a GO enrichment analysis based on the result of the search against the Nr database by the hypergeometric test (Supplementary Data 6). DEGs were enriched into 41 GO terms of which 27 terms including 'binding,' 'catalytic activity,' 'organelle,' 'cell part' were both enriched for the four DEGs sets. Additionally, 3 GO terms including 'electron carrier activity,' 'transporter activity,' and 'structural molecule activity' were enriched for DEGs of 'J1_vs_A1', while DEGs from 'A0_vs_A1' and 'J0_vs_J1' were both

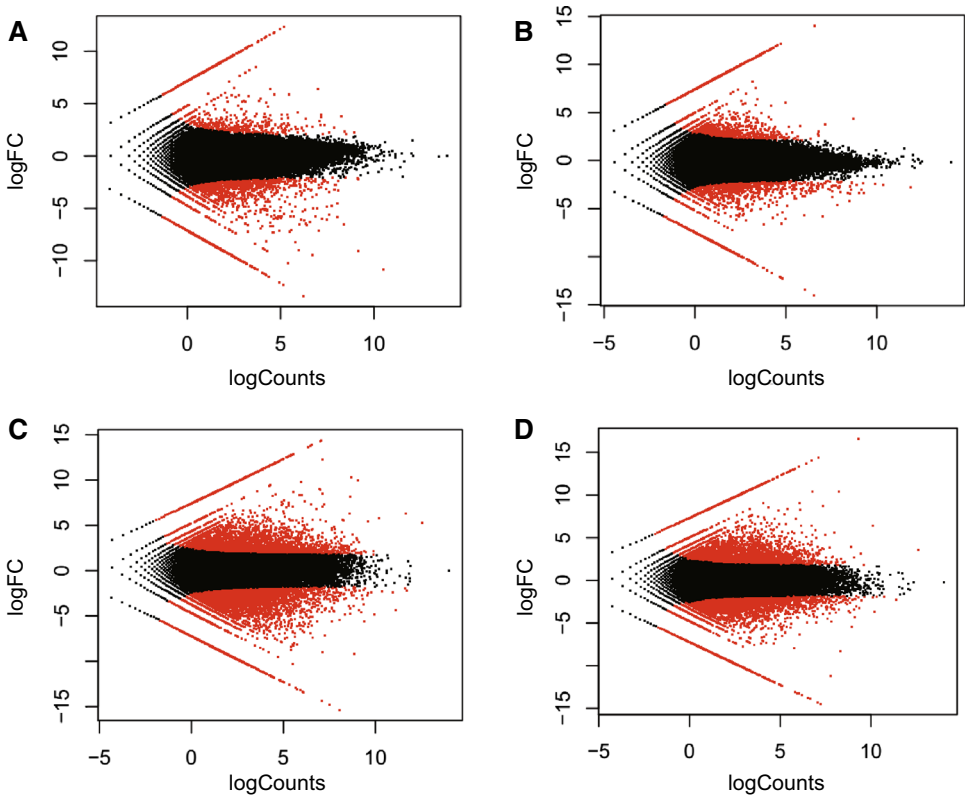

Fig. 6 Log-fold changes in gene expression. **a** Log-fold changes in gene expression in 'J1_vs_A1'. **b** Log-fold changes in gene expression in 'J0_vs_A0'. **c** Log-fold changes in gene expression in 'J0_vs_A0'. **d** Log-fold changes in gene expression in 'A0_vs_A1'

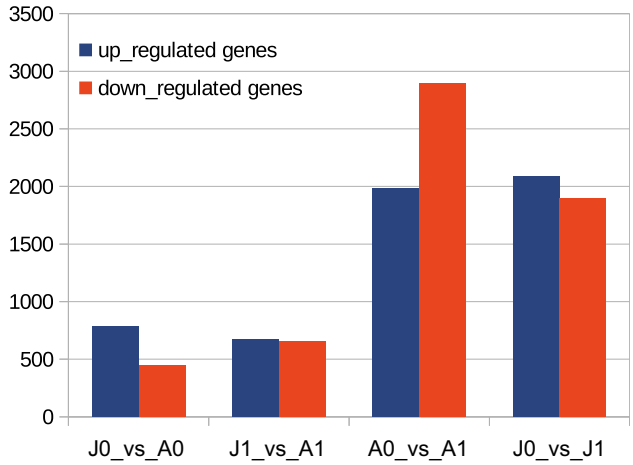

Fig. 7 Differently expressed genes between *A. fasciata* juvenile and adult plants. 'J1_vs_A1' refers to the comparison between the juvenile and adult plant with ethylene treatment; 'J1_vs_A0' refers to the comparison between the juvenile and adult plant with water treatment; 'J0_vs_J1' refers to the comparison between the juvenile plant with water and ethylene treatment; 'A0_vs_A1' refers to the comparison between the adult plant with water and ethylene treatment; "P value < 0.001, the absolute value of Log2 fold change (Log2 FC) ≥ 2 and FPKM ≥ 1" were used as the threshold to determine the significance of gene expression differences

enriched into the categories of 'electron carrier activity,' 'membrane-enclosed lumen,' 'cell junction,' 'symplast,' 'transporter activity,' and 'growth.'

To detect the pathways that DEGs were involved in, we carried out KEGG enrichment analysis. After the DEG sequences were searched against the KEGG database, DEGs were assigned into KEGG pathways. And the KEGG pathways were then assigned corrected p-values through the hypergeometric test. A total of 57 KEGG pathways were represented, of which 5 pathways including 'Metabolic pathways,' 'Biosynthesis of secondary metabolites,' 'ABC transporters,' 'Plant-pathogen interaction,' and 'Spliceosome' were enriched for the four DEGs sets. Comparing to DEGs in 'J0_vs_A0,' DEGs in 'J1_vs_A1' were enriched in 'Phenylpropanoid biosynthesis,' 'Plant hormone signal transduction,' 'Other glycan degradation,' 'Isoquinoline alkaloid biosynthesis,' 'Phenylalanine, tyrosine and tryptophan biosynthesis,' 'Starch and sucrose metabolism,' 'Valine, leucine and isoleucine biosynthesis,' 'Cutin, suberine and wax biosynthesis,' and 'Carotenoid biosynthesis,' while DEGs in 'J0_vs_A0' were not represented. Meanwhile, DEGs in 'A1_vs_J1' and 'A0_vs_A1' were also both enriched into 'Glycerophospholipid metabolism,' 'Endocytosis,' 'Ether lipid metabolism,' 'NA transport,' and so on; totally 10 pathways except the 5 pathways that the four DEGs set were both represented in, while a total of 24 pathways including 'Pyrimidine metabolism,' 'RNA polymerase,' 'Phenylpropanoid biosynthesis,' 'Glycolysis/Gluconeogenesis,' etc., that DEGs in 'A1_vs_J1' were enriched into but DEGs in 'A0_vs_A1' were not (Supplementary Data 7).

DEGs Involved in Flowering

We indentified 62 DEGs that may be involved in flowering from our transcriptome data (Table 2, Supplementary Data 8). These DEGs included several pathway genes that control flowering time and flowering development: (1) ethylene signaling pathway elements *EIN4*, *CTR1*, *Ethylene-overproduction protein 1* (*ETO1*), and *EIL3*; (2) photoperiodic pathway and circadian clock-related genes, *CO*, *GI*, *CRY2*, *LATE ELONGATED HYPOCOTYL* (*LHY*), *COP1*, and *HAP3*; (3) AP2/ERF family genes, AP2-like ethylene-responsive TF *At2g41710*, *TOE1*, *TOE2*, *TOE3*, *ERF Win1*, *ERF 1*, *ERF 109*, and *ERF 014*; MADS-box family genes, *MADS-box 14*, *MADS-box 23*, and *MADS-box 5*; (4) E3 ubiquitin ligase-related genes, *COP1*, *Cullin-1*, and F-box family proteins; (5) PHYTOCHROME-INTERACTING FACTORs, *PIF3* and *PIF4*; (6) GA pathway genes, *GA2ox*, *GA20ox*, *GID1*, and *DELLA*; (7) floral organ and meristem identity genes, *APETALA 1* (*AP1*) and *AGAMOUS* (*AG*); (8) other genes involve in flowering timing and development, *alpha, alpha-trehalose-phosphate synthase* (*TPS6*, *TPS7*, *TPS9*), *FD*, *CLAVATA 1* (*CLV1*), *BEL1*, *cytochrome P450 90B1*, *cytochrome P450 734A6*, serine/threonine-protein kinase *BRI1*, and *ULTRAPETALA 1* (*UTL1*). According to the expression patterns of these DEGs, we classified these DEGs into three classes: (1) DEGs expressed differently in 'J0_vs_A0,' including *COL3*, *PIN2*, *TOE3*, *CRY2*, and so on; (2) DEGs expressed differently in 'J1_vs_A1,' including *FT*, *TPS6*, *HAP3*, *GA2OX8*, *CTR1*, *CRY2,* and so on; (3) DEGs expressed differently in 'A0_vs_A1' or 'J0_vs_J1' but not in 'J0_vs_A0' and 'A1_vs_A0,' including, *WIN1*, *EIN4*, *ACC synthase 1*, *GID1*, *PIF3*, *BRI1*, etc. Theoretically, the first class of DEGs may be involved in development of *A. fasciata*; the second class of DEGs may play key roles in flowering induction by ethylene in adult *A. fasciata* plants. The third class of DEGs may participate in the basic response of ethylene.

Of the DEGs involving flowering, 13 DEGs were selected to qRT-PCR analysis (Fig. 8, Supplementary Data 9). The expression of selected DEGs was examined in adult and juvenile plants under water and ethylene treatment, respectively. c2000030287_g1_i1 (*FT*), c100007569_g2_i1 (*GI*), c100001514_g3_i1 (*AP1*), and c2000048950_g1_i1 (*MADS5*) both increased in adult and juvenile plants under ethylene treatment compared to plants with water treatment, but increased more markedly in adult plants with ethylene treatment. c2000016847_g1_i1 (*FD*) and c100001523_g5_i1 (*AP2*) decreased both in adult and juvenile plants under ethylene treatment. The expression of these DEGs was analyzed by qRT-PCR corresponding with expression level in comparative transcriptome analysis, suggesting that the transcriptome profiles accurately reflected global transcriptome changes in response to ethylene treatment.

Discussion

We have performed comparative transcriptome analysis of two libraries from adult and juvenile plants under ethylene treatment in our previous study, with 52,560,902 and 52,396,972 Illumina clean reads, respectively. In this study, we constructed four transcriptome libraries of *A. fasciata* adult and juvenile plants under water and ethylene treatment, and achieved totally 86,609 sequences with a mean size of 987 bp, whereas we obtained a library of 71,445 unique sequences with a mean length of 461 bp in our previous study. Using BlastX to search against the Nr database with a cut-off E-value of 1e-5, 49,423 genes (57.06 % of unigene sequences) resulted in a significant hit; however, 35,483 genes (49.7 % of the unigene sequences) were matched to the Nr database in the previous study. With the more clean reads, we constructed a more complete and accurate transcriptome library, which will fascinate further analysis. Moreover, we obtained 10,036 DEGs between adult and juvenile plants under ethylene treatment in our previous study, which is more than the 1328 DEGs in this study, indicating that we reduced false positive predictions markedly in our DEG analysis.

ACC synthase is a key enzyme in ethylene synthesis and a key contributor toward flowering in mature pineapple (Trusov and Botella 2006). ACC synthase was upregulated in both 'A0_vs_A1' and 'J0_vs_J1,' implying that both adult and juvenile plants responded to ethylene by a burst of endogenous ethylene synthesis (Trusov and Botella 2006). *FT* protein is the major component of the mobile flower-promoting signal florigen, promoting the transition from vegetative growth to flowering in plants. Our data implying that the abundance of *FT* increased both in adult and juvenile plants in response to ethylene and dramatically increased in adult plants. After expression in leaves, *FT* proteins were transferred to the shoot apex and interacted with *FD*, resulting in increased expression of *AP1* in the shoot apex and inducing subsequent flowering. *FD* is a TF required for transition to flowering promoted by *FT* (Abe and others 2005). *FD* is already expressed before floral induction in vegetative growing tissue and preferentially expressed in the shoot apex. *FD* mRNA was observed in leaf and floral anlagen, and was reduced soon after *AP1* was expressed (Wigge and others 2005). The decrease of *FD* in our transcriptome data both in adult and juvenile plants may be associated with increasing abundance of *FT* protein in the shoot apex. The increased *AP1* expression level and decreased abundance of *FD* mRNA in our transcriptome data suggested that the increased *FT*

Table 2 Differently expressed genes involved in *A. fasciata* flowering

	Unigene	Homolog genes	Homolog genes ID	*e* value
Class 1	c100006396_g1_i1	CONSTANS-like 3-Like protein [*Musa acuminata* subsp. *malaccensis*]	ref|XP_009418181.1	2E−30
	c100003104_g3_i1	Auxin efflux carrier component 2 [*Phoenix dactylifera*]	ref|XP_008781803.1	5E−126
	c100009256_g1_i1	Transcription factor PIF4-like [*Musa acuminata* subsp. *malaccensis*]	ref|XP_009399053.1	2E−55
	c100003238_g5_i1	Cryptochrome 2 [*Oryza sativa* Indica Group]	gi|23954324	1E−135
	c100003130_g1_i1	Protein LHY [*Arabidopsis thaliana*]	sp|Q6R0H1	3E−78
	c100002614_g6_i1	AP2-like ethylene-responsive transcription factor At2g41710 [*Arabidopsis thaliana]*	ref|XP_008809562.1	3E−99
	c100002614_g16_i1	AP2-like ethylene-responsive transcription factor At2g41710 [*Arabidopsis thaliana*]	ref|XP_008809562.1	2E−84
	c100009180_g1_i1	ethylene-responsive transcription factor ERF109-like [*Arabidopsis thaliana*]	sp|Q9SZ06	4E−39
	c2000036455_g1_i1	AP2 like ethylene-responsive transcription factor TOE3[*Phoenix dactylifera*]	ref|XP_008789029.1	5E−148
Class 2	c2000030287_g1_i1	FT-like protein [*Musa acuminata* subsp. *malaccensis*]	ref|XP_009389899.1	2E−69
	c100008356_g3_i1	cytochrome P450 90B1-like [*Phoenix dactylifera*]	ref|XP_008778138.1	0
	c100006890_g1_i1	gibberellin 2-oxidase 3 [*Spinacia oleracea*]	gb|AAX14674.1	1E−68
	c100006890_g4_i1	gibberellin 2-beta-dioxygenase 8-like [*Fragaria vesca* subsp. *vesca*]	Gi|470118260	4E−105
	c100002594_g2_i1	F-box family protein [*Populus trichocarpa*]	gi|224078846	0
	c100002594_g1_i1	F-box family protein [*Populus trichocarpa*]	gi|224078846	0
	c2000028559_g1_i1	HAP3 subunit of HAP complex [*Oryza sativa* Japonica Group]	gi|115473263	2E−62
	c100008591_g7_i1	MADS-BOX transcription factor 23-like [*Phoenix dactylifera*]	ref|XP_008800745.1	3E−42
	c10000268_g1_i1	Serine/threonine-protein kinase CTR1 [*Phoenix dactylifera*]	ref|XP_008802316.1	0
	c100002614_g2_i1	AP2-like ethylene-responsive transcription factor At2g41710 [*Arabidopsis thaliana*]	ref|XP_008809562.1	1E−108
	c100001523_g5_i1	AP2 like ethylene-responsive transcription factor TOE3 [*Phoenix dactylifera*]	ref|XP_008789029.1	2E−135
	c100002875_g4_i1	Alpha,alpha-trehalose-phosphate synthase [UDP-forming] 6 [*Arabidopsis thaliana*]	sp|Q94AH8	0
	c2000024402_g1_i1	Cullin-1 [*Arabidopsis thaliana*]	sp|Q94AH6	0
	c100001514_g4_i1	apetala1/squamosa protein [*Alstroemeria ligtu* subsp. *ligtu*]	gi|379698673	5E−85
	c100001514_g2_i1	apetala1/squamosa protein [*Alstroemeria ligtu* subsp. *ligtu*]	gi|379698673	6E−25
	c2000039574_g1_i1	AGAMOUS-like MADS-BOX protein [*Cocos nucifera*]	gb|AIK66813.1	7E−119
Class 3	c200009394_g1_i1	Protein EIN4 [*Phoenix dactylifera*]	ref|XP_008787409.1	0
	c2000034193_g1_i1	DELLA protein GAI-like [*Phoenix dactylifera*]	Ref|XP_008777332.1	1E−112
	c2000020552_g1_i1	Ethylene-responsive transcription factor WIN1[*Phoenix dactylifera*]	ref|XP_008804592.1	2E−73
	c2000017349_g1_i1	Serine/threonine-protein kinase BRI1-like 1[*Arabidopsis thaliana*]	sp|Q9ZWC8	1E−107
	c100009185_g1_i1	Transcription factor PIF3 [*Arabidopsis thaliana*]	sp|O80536	2E−57
	c100006331_g2_i1	cytochrome P450 734A6-like [*Phoenix dactylifera*]	ref|XP_008805359.1	0
	c100002863_g3_i1	1-aminocyclopropane-1-carboxylate synthase 1 [*Prunus mume*]	sp|Q9MB95	0
	c100002328_g3_i1	Gibberellin receptor GID1[*Oryza sativa* Japonica Group]	sp|Q6L545	2E−108
	c100001514_g3_i1	apetala1/squamosa protein [*Alstroemeria ligtu* subsp. *ligtu*]	gi|379698673	7E−85
	c100001514_g1_i1	apetala1/squamosa protein [*Alstroemeria ligtu* subsp. *ligtu*]	gi|379698673	5E−25
	c200006263_g1_i1	protein ABSCISIC ACID-INSENSITIVE 5-like [*Musa acuminata* subsp. *malaccensis*]	ref|XP_009411951.1	1E−34
	c2000045781_g1_i1	Transcription factor PIF-4 like [*Phoenix dactylifera*]	ref|XP_008811826.1	8E−42
	c2000029127_g1_i1	Ethylene-responsive transcription factor 1B, putative [*Ricinus communis*]	gi|255581463	5E−48
	c20000278_g1_i1	Probable alpha, alpha-trehalose-phosphate synthase [UDP-forming] 7 [*Arabidopsis thaliana*]	sp|Q9LMI0	0
	c10000843_g1_i1	Protein SUPPRESSOR OF PHYA-105 1 [*Arabidopsis thaliana*]	sp|Q9SYX2	2E−177
	c100007569_g2_i1	Protein GIGANTEA [*Oryza sativa* Japonica Group]	gi|115434924	0
	c100006475_g2_i1	Ubiquitin ligase protein COP1[*Arabidopsis thaliana*]	gi|413939110	0

Table 2 continued

Unigene	Homolog genes	Homolog genes ID	*e* value
c100003459_g1_i1	Protein FD [*Arabidopsis thaliana*]	gi|225457875	2E−19
c100002614_g9_i1	AP2-like ethylene-responsive transcription factor At2g41710 [*Arabidopsis thaliana*]	ref|XP_008809562.1	2E−76
c200008580_g1_i1	gibberellin 20-oxidase, putative [*Musa balbisiana*]	gi|102139962	1E−117
c20000669_g1_i1	Ethylene-overproduction protein 1[*Phoenix dactylifera*]	ref|XP_008789159.1	0
c2000048950_g1_i1	MADS5 protein [*Dendrocalamus latiflorus*]	gi|47681327	3E−60
c2000048320_g1_i1	Protein ULTRAPETALA 1[*Vitis vinifera*]	sp|Q8GZA8	8E−88
c2000016847_g1_i1	Protein FD [*Arabidopsis thaliana*]	sp|Q84JK2	5E−20
c2000012974_g1_i1	Ethylene-responsive transcription factor ERF014 [*Arabidopsis thaliana*]	sp|Q9LPE8	5E−34
c100009185_g2_i1	Transcription factor PIF3 [*Arabidopsis thaliana*]	sp|O80536	2E−57
c100008827_g2_i1	bel1 homeotic protein, putative [*Ricinus communis*]	gi|255537553	1E−135
c100008591_g5_i1	MADS-BOX transcription factor 23-like [*Nicotiana tomentosiformis*]	ref|XP_009595409.1	4E−26
c10000859_g2_i1	Probable alpha, alpha-trehalose-phosphate synthase [UDP-forming] 9 [*Arabidopsis thaliana*]	sp|Q9LRA7	0
c100007967_g1_i1	Ethylene-responsive transcription factor 1[*Oryza sativa* Japonica Group]	sp|Q6K7E6	9E−60
c100007087_g2_i1	ETHYLENE INSENSITIVE 3-like 3 protein [*Arabidopsis thaliana*]	sp|O23116	2E−140
c100007087_g1_i1	ETHYLENE INSENSITIVE 3-like 3 protein [*Arabidopsis thaliana*]	sp|O23116	2E−140
c100005536_g1_i1	Receptor protein kinase CLAVATA1 [*Arabidopsis thaliana*]	sp|Q9SYQ8	5E−67
c100005525_g5_i1	DELLA protein DWARF8 [*Zea mays*]	sp|Q9ST48.1	0
c100005525_g1_i1	DELLA protein DWARF8 [*Zea mays*]	sp|Q9ST48.1	3E−114
c100004788_g1_i1	MADS-box transcription factor 14-like [*Phoenix dactylifera*]	ref|XP_008794203.1	2E−61
c100001523_g8_i1	Ethylene-responsive transcription factor RAP2-7-like [*Phoenix dactylifera*]	ref|XP_008789031.1	1E−121

The DEGs related with flowering were theoretically classed into three classes according to expression type of the DEGs. *Class 1* DEGs may be involved in development of *A. fasciata*, *Class 2* DEGs may be involved in the flowering induction by ethylene in adult *A. fasciata* plants, *Class 3* DEGS may be involved in the basic response of ethylene

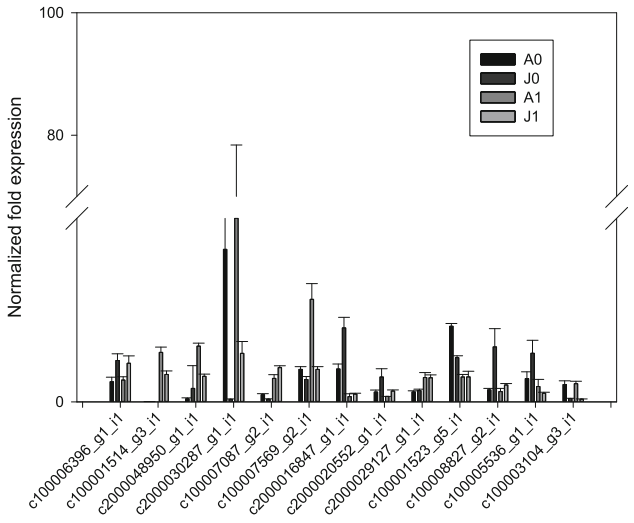

Fig. 8 qRT-PCR validation of selected differently expressed genes. The amount of transcript was normalized to the level of *A. fasciata* actin like gene (homolog with *Ananas comosus* action gene gi\|397881472). Mean values and standard errors (*bars*) were obtained from three biological replicates and three technical replicates

expression in leaves resulted in flowering induction in *A. fasciata* adult plants with ethylene treatment.

The photoperiod pathway controls the response to seasonal day length and acts in the leaves through a signaling cascade involving *GI* and the transcriptional regulator *CO*. The circadian clock controls the floral transition in many species. *CIRCADIAN CLOCK ASSOCIATED1* (*CCA1*), *LHY*, and *TIMING OF CAB EXPRESSION1* (*TOC1*) act as crucial players in regulation of the circadian clock. *LHY* is a negative regulator of *TOC1* and *PSEUDO RESPONSE REGULATORS 1* (*PRR1*) (Pineiro and Jarillo 2013). *TOC1* acts as a negative regulator of *GI* (Bolouri Moghaddam and den Ende 2013). The abundance of *LHY* mRNA was downregulated in 'J0_vs_A0.' Further, our data showed that the abundance of *GI* expression was significantly increased under ethylene treatment in *A. fasciata*. *GI* positively regulated the expression of *CO*. The blue light photoreceptor cryptochrome *CRY2* is upregulated in 'A1_vs_J1' and 'A0_vs_J0,' which may positively regulate the stability of *CO*. So, the increasing expression level of

key photoperiodic pathway genes *GI* and *CRY2* may result in increasing abundance of *CO* protein and upregulate *FT* transcription. *CO* bound with *HAP3* and *HAP5* through the CCT motif promotes flowering by enhancing expression of *FT* and SUPPRESSOR OF CONSTANS1 (SOC1) (Cai and others 2007; Wenkel and others 2006). *HAP3* was highly upregulated in 'A0_vs_J0' and 'A0_vs_A1,' which could be the partial reason of the increased expression of *FT*. In summary, our data imply that genes in the photoperiod pathway play a key role in flowering induction by ethylene in *A. fasciata*.

FT acts as an integrator, merging various environmental and developmental cues such as temperature, photoperiod, GA, and plant age. The *AP2* family, acting as repressors of *FT*, is also downregulated in 'A0_vs_J0,' including *TOE1* and *TOE3*. *TOE1* and *TOE3* are the targets of miR172 and repressed by miR172. miR172 reduces the abundance of its targets. Additionally, *GI* is involved in this photoperiodic miR172 induction (Jung and others 2007). The increased abundance of *GI* may result in the amount of miR172 increasing. *TOE1* and *TOE3* and miR172 were correlated with plant development stages (Song and others 2013). Therefore, the *AP2* family may result in the different response of *A. fasciata* adult and juvenile plants to ethylene treatment.

Regulation of GA concentration is primarily via the biosynthesis enzymes *GA20ox* and *GA3ox*, and inactivating enzymes *GA2ox*. *GA20ox* was upregulated and *GA20x* downregulated in 'A1_vs_J1,' indicating that the bioactive GAs increased in adult plants with ethylene treatment. Bioactive GAs promote binding of the *GID1* receptor to *DELLA* and initiate *DELLA* degradation (Mutasa-Gottgens and Hedden 2009). *DELLA* reduces the amount of miR172 and represses the activator of *FT*, including *SPL3*, *SPL4*, and *SPL5*. *DELLA* also negatively regulates *PIF4* activity, which activates the expression of *FT* under high temperatures (de Lucas and others 2008). It is suggested that *DELLA* proteins mediate transcriptional activation of the *GID1*, *GA20ox*, and *GA3ox* genes and the repression of *DELLA* transcription (Middleton and others 2012). The decreasing concentration of *DELLA* protein may lead to decreased *GID1* expression. *GID1* was downregulated in both 'A0_vs_A1' and 'J0_vs_J1,' suggesting that both adult and juvenile plants increased the synthesis of bioactive GA, resulting in decreased *DELLA* protein abundance. Additionally, BRs and ABA influence flowering time by regulating *FLC*. ABA inhibits flower transition by *ABI5*, which was downregulated in our data (Wang and others 2013). The differential expression of *cytochrome P450 90B1*, *cytochrome P450 734A6*, *BRI1*, and *ABI5* in our transcriptome data indicated that ABA and BRs were also influenced by ethylene in the process of flowering induction by ethylene.

Trehalose-6-phosphate has been proposed to function as a proxy for carbohydrate status of plants and plays a key role in the presence of excess sugar (Matsoukas 2014). Plants integrate diverse environmental and endogenous signals to ensure the timely transition from vegetative growth to flowering (Wahl and others 2013). Tre6P is required for *FT* and *TSF* expression under an inductive photoperiod. *TPS7* and *TPS9* were upregulated in 'A0_vs_A1' and 'J0_vs_J1,' suggesting the abundance of Tre6p increased in response to ethylene. Recent studies suggested that ethylene and sugar may interplay by the *GID1* and *PIF* family (Matsoukas 2014). Hence, the interplay between sugar and ethylene may influence flowering induction in *A. fasciata*.

It is proposed that *AGAMOUS* (*AG*) is involved in the control of organ identity during early development of flowers and acts as a C class cadastral protein through repressing A class floral homeotic genes such as *APETALA1*. *TOE3* binds to the second intron of the *AG* gene (Jung and others 2014). *Clavata1* (*CLV1*) and *BEL1* act with *CLV3* in a signal transduction pathway coordinating growth between adjacent meristematic regions and control the balance between meristem cell proliferation and differentiation. *BEL1* also acts with *SHOOT MERISTEMLESS*, formatting the *BEL1–STM* complex to maintain the indeterminacy of the inflorescence meristem (Bellaoui and others 2001). The differential expression of *AG*, *APETELA1*, *CLV1*, and *BEL1* implied that the arrival of FT in the shoot apex meristem initiated the transition from vegetative to reproductive development in *A. fasciata*.

It has been revealed that ethylene signaling interacts with the GA pathway by reducing endogenous levels of GAs (Davis 2009). Ethylene causes stabilization of *EIN3* and *EIN3-like* proteins by inhibiting the activity of their protease *SCF* (Binder and others 2007). But our data indicated that bioactive GAs were increased under ethylene treatment. So, how GA and ethylene interplay in *A. fasciata* remains unclear and worth studying. Moreover, the mechanism of the *AP2* family response to ethylene in *A. fasciata* needs further study.

Conclusions

This study provided a global survey of changes in transcriptomes of *A. fasciata* in response to ethylene. The analyses of transcriptome profiles imply that *FT* is upregulated markedly in the adult plant and resulted in flowering. The AP2 family genes, such as *TOE1* and *TOE3*, may result in age-dependent flowering induction by ethylene. Moreover, the differential expressions of *GI*, *DELLA*, *GAD1,* and so on indicate that a complicated network participated in the induction of flowering by ethylene, which will help in future studies.

Acknowledgments The research was supported by the The National Natural Science Foundation of China (31372106) and The Fundamental Scientific Research Funds for CATAS-TCGRI (163003 2014018).

References

Abe M, Kobayashi Y, Yamamoto S, Daimon Y, Yamaguchi A, Ikeda Y et al (2005) FD, a bZIP protein mediating signals from the floral pathway integrator FT at the shoot apex. Science 309:1052–1056

Achard P, Baghour M, Chapple A, Hedden P, Van Der Straeten D, Genschik P et al (2007) The plant stress hormone ethylene controls floral transition via DELLA-dependent regulation of floral meristem-identity genes. Proc Natl Acad Sci USA 104:6484–6489

Andres F, Coupland G (2012) The genetic basis of flowering responses to seasonal cues. Nat Rev Genet 13:627–639

Aukerman MJ, Sakai H (2003) Regulation of flowering time and floral organ identity by a MicroRNA and its APETALA2-like target genes. Plant Cell 15:2730–2741

Bellaoui M, Pidkowich MS, Samach A, Kushalappa K, Kohalmi SE, Modrusan Z et al (2001) The *Arabidopsis* BELL1 and KNOX TALE homeodomain proteins interact through a domain conserved between plants and animals. Plant cell 13:2455–2470

Binder BM, Walker JM, Gagne JM, Emborg TJ, Hemmann G, Bleecker AB et al (2007) The *Arabidopsis* EIN3 binding F-Box proteins EBF1 and EBF2 have distinct but overlapping roles in ethylene signaling. Plant Cell 19:509–523

Bolouri Moghaddam MR, den Ende WV (2013) Sugars, the clock and transition to flowering. Fron Plant Sci 4:22. doi:10.3389/fpls.2013.00022

Boyle EI, Weng S, Gollub J, Jin H, Botstein D, Cherry JM et al (2004) GO:TermFinder–open source software for accessing Gene Ontology information and finding significantly enriched Gene Ontology terms associated with a list of genes. Bioinformatics 20:3710–3715

Cai X, Ballif J, Endo S, Davis E, Liang M, Chen D et al (2007) A putative CCAAT-binding transcription factor is a regulator of flowering timing in *Arabidopsis*. Plant Physiol 145:98–105

Chuck G, Hake S (2005) Regulation of developmental transitions. Curr Opin Plant Biol 8:67–70

Conesa A, Gotz S, Garcia-Gomez JM, Terol J, Talon M, Robles M (2005) Blast2GO: a universal tool for annotation, visualization and analysis in functional genomics research. Bioinformatics 21:3674–3676

Davis SJ (2009) Integrating hormones into the floral-transition pathway of *Arabidopsis thaliana*. Plant Cell Environ 32:1201–1210

de Lucas M, Daviere JM, Rodriguez-Falcon M, Pontin M, Iglesias-Pedraz JM, Lorrain S et al (2008) A molecular framework for light and gibberellin control of cell elongation. Nature 451:480–484

Fornara F, de Montaigu A, Coupland G (2010) SnapShot: control of flowering in *Arabidopsis*. Cell 141:550 e551–550 e552

Galvao VC, Horrer D, Kuttner F, Schmid M (2012) Spatial control of flowering by DELLA proteins in *Arabidopsis thaliana*. Development 139:4072–4082

Grabherr MG, Haas BJ, Yassour M, Levin JZ, Thompson DA, Amit I et al (2011) Full-length transcriptome assembly from RNA-Seq data without a reference genome. Nat Biotechnol 29:644–652

Hua J, Meyerowitz EM (1998) Ethylene responses are negatively regulated by a receptor gene family in *Arabidopsis thaliana*. Cell 94:261–271

Iseli C, Jongeneel CV, Bucher P (1999) ESTScan: a program for detecting evaluating and reconstructing potential coding regions in EST sequences. ISMB 99:138–148

Jung JH, Seo YH, Seo PJ, Reyes JL, Yun J, Chua NH et al (2007) The GIGANTEA-regulated microRNA172 mediates photoperiodic flowering independent of CONSTANS in *Arabidopsis*. Plant Cell 19:2736–2748

Jung CH, Wong CE, Singh MB, Bhalla PL (2012) Comparative genomic analysis of soybean flowering genes. PLoS One 7:e38250

Jung JH, Lee S, Yun J, Lee M, Park CM (2014) The miR172 target TOE3 represses AGAMOUS expression during *Arabidopsis* floral patterning. Plant Sci 215–216:29–38

Kieber JJ, Rothenberg M, Roman G, Feldmann KA, Ecker JR (1993) CTR1, a negative regulator of the ethylene response pathway in Arabidopsis, encodes a member of the raf family of protein kinases. Cell 72:427–441

Kumar SV, Lucyshyn D, Jaeger KE, Alos E, Alvey E, Harberd NP et al (2012) Transcription factor PIF4 controls the thermosensory activation of flowering. Nature 484:242–245

Langmead B, Trapnell C, Pop M, Salzberg SL (2009) Ultrafast and memory-efficient alignment of short DNA sequences to the human genome. Genome Biol 10:R25

Lingam S, Mohrbacher J, Brumbarova T, Potuschak T, Fink-Straube C, Blondet E et al (2011) Interaction between the bHLH transcription factor FIT and ETHYLENE INSENSITIVE3/ETHYLENE INSENSITIVE3-LIKE1 reveals molecular linkage between the regulation of iron acquisition and ethylene signaling in *Arabidopsis*. Plant Cell 23:1815–1829

Livak KJ, Schmittgen TD (2001) Analysis of relative gene expression data using real-time quantitative PCR and the $2 - \Delta\Delta CT$ method. Methods 25:402–408

Mao X, Cai T, Olyarchuk JG, Wei L (2005) Automated genome annotation and pathway identification using the KEGG Orthology (KO) as a controlled vocabulary. Bioinformatics 21:3787–3793

Matsoukas IG (2014) Interplay between sugar and hormone signaling pathways modulate floral signal transduction. Frontiers in genetics 5:218

Merchante C, Alonso JM, Stepanova AN (2013) Ethylene signaling: simple ligand, complex regulation. Curr Opin Plant Biol 16:554–560

Middleton AM, Ubeda-Tomas S, Griffiths J, Holman T, Hedden P, Thomas SG et al (2012) Mathematical modeling elucidates the role of transcriptional feedback in gibberellin signaling. Proc Natl Acad Sci USA 109:7571–7576

Mortazavi A, Williams BA, McCue K, Schaeffer L, Wold B (2008) Mapping and quantifying mammalian transcriptomes by RNA-Seq. Nat Methods 5:621–628

Mutasa-Gottgens E, Hedden P (2009) Gibberellin as a factor in floral regulatory networks. J Exp Bot 60:1979–1989

Pfaffl MW (2001) A new mathematical model for relative quantification in real-time RT–PCR. Nucleic Acids Res 29:e45

Pineiro M, Jarillo JA (2013) Ubiquitination in the control of photoperiodic flowering. Plant science : an international journal of experimental plant biology 198:98–109

Robinson MD, McCarthy DJ, Smyth GK (2010) edgeR: a Bioconductor package for differential expression analysis of digital gene expression data. Bioinformatics 26:139–140

Sawa M, Kay SA (2011) GIGANTEA directly activates Flowering Locus T in *Arabidopsis thaliana*. Proc Natl Acad Sci USA 108:11698–11703

Schaller GE (2012) Ethylene and the regulation of plant development. BMC Biol 10:9

Solano R, Stepanova A, Chao Q, Ecker JR (1998) Nuclear events in ethylene signaling: a transcriptional cascade mediated by

ETHYLENE-INSENSITIVE3 and ETHYLENE-RESPONSE-FACTOR1. Genes Dev 12:3703–3714

Song YH, Ito S, Imaizumi T (2013) Flowering time regulation: photoperiod- and temperature-sensing in leaves. Trends Plant Sci 18:575–583

Trusov Y, Botella JR (2006) Silencing of the ACC synthase gene ACACS2 causes delayed flowering in pineapple [*Ananas comosus* (L.) Merr.]. J Exp Bot 57:3953–3960

Wahl V, Ponnu J, Schlereth A, Arrivault S, Langenecker T, Franke A et al (2013) Regulation of flowering by trehalose-6-phosphate signaling in *Arabidopsis thaliana*. Science 339:704–707

Wang Y, Li L, Ye T, Lu Y, Chen X, Wu Y (2013) The inhibitory effect of ABA on floral transition is mediated by ABI5 in *Arabidopsis*. J Exp Bot 64:675–684

Wenkel S, Turck F, Singer K, Gissot L, Le Gourrierec J, Samach A et al (2006) CONSTANS and the CCAAT box binding complex share a functionally important domain and interact to regulate flowering of *Arabidopsis*. Plant Cell 18:2971–2984

Wigge PA, Kim MC, Jaeger KE, Busch W, Schmid M, Lohmann JU et al (2005) Integration of spatial and temporal information during floral induction in *Arabidopsis*. Science 309:1056–1059

Wu G, Park MY, Conway SR, Wang JW, Weigel D, Poethig RS (2009) The sequential action of miR156 and miR172 regulates developmental timing in *Arabidopsis*. Cell 138:750–759

Yu S, Galvao VC, Zhang YC, Horrer D, Zhang TQ, Hao YH et al (2012) Gibberellin regulates the *Arabidopsis* floral transition through miR156-targeted SQUAMOSA promoter binding-like transcription factors. Plant Cell 24:3320–3332

Zhong S, Zhao M, Shi T, Shi H, An F, Zhao Q et al (2009) EIN3/EIL1 cooperate with PIF1 to prevent photo-oxidation and to promote greening of *Arabidopsis* seedlings. Proc Natl Acad Sci USA 106:21431–21436

Zuo Z, Liu H, Liu B, Liu X, Lin C (2011) Blue light-dependent interaction of CRY2 with SPA1 regulates COP1 activity and floral initiation in *Arabidopsis*. Curr Biol 21:841–847